Am J Transl Res 2020;12(8):4384-4396
www.ajtr.org /ISSN:1943-8141/AJTR0108876

Original Article

Telocytes enhanced in vitro decidualization and mesenchymal-epithelial transition in endometrial stromal cells via Wnt/β-catenin signaling pathway

Fei-Lei Zhang, Yue-Lin Huang, Xiao-Ye Zhou, Xue-Ling Tang, Xiao-Jun Yang

Department of Obstetrics and Gynecology, The First Affiliated Hospital of Soochow University, Suzhou 215006, Jiangsu Province, PR China

Received February 8, 2020; Accepted July 4, 2020; Epub August 15, 2020; Published August 30, 2020

Abstract: Decidualization of endometrial stromal cells (ESCs) is essential for preparing endometrium for embryo implantation. Telocytes (TCs), a novel type of interstitial cell, exist in the female reproductive tract and participate in the pathophysiology of diseases. This study further investigates the hypothesis that TCs, a source of Wnt, modulates decidualization and MET in ESCs. We had observed differential expression of Wnt ligands in primary mice ESCs and TCs by qPCR. TCM-induced decidualization and MET was assessed in ESCs. Changes in markers for decidualization (cyclin-D3, desmin, d/tPRP), stromal cells (N-cadherin), epithelial cells (E-cadherin), and the Wnt/β-catenin pathway (β-catenin, FOXO1) were quantified by western blot and RT-PCR. β-catenin knockdown in ESCs decreased the degree of TCM-induced decidualization and MET, with significantly reversed expression profiles ($P < 0.05$). This is the first study to show that TCs can enhance decidualization and MET in ESCs through the Wnt/β-catenin signaling-pathway. Therefore, we describe a promising cell therapy for gynecological conditions and related reproductive problems associated with defective decidualization.

Keywords: Telocytes (TCs), endometrial stromal cells (ESCs), decidualization, mesenchymal-epithelial transition (MET), Wnt/β-catenin signaling-pathway

Introduction

Telocytes (TCs) are a novel type of interstitial cell first identified by Popescu et al. in 2010 [1]. They are described as having a small cell body with extremely long extensions named telopodes (Tps), with alternating thin (podomers) and thick segments (podoms) [2]. The proposed functions of TCs were based on its characteristic Tps feature. TCs form a three-dimensional network within interstitial tissues using Tps, with various intercellular junctions with adjacent cells to directly influence their activities. In addition, TCs releasing paracrine signaling substances, such as exosomes and/or vesicles to regulate nearby cells [3-5]. TCs have been documented in various mammalian organs and tissues (such as heart, lung, pancreas, skin, skeletal muscle, urinary system, liver, and trigeminal ganglion [6-8]. TCs also have several potential functions, such as tissue regeneration and repair, intercellular signaling, and nursing of stem cell niches and immature cells during organogenesis [9]. TCs were also found in female reproductive organs and tissues including the uterus, oviduct, and placenta, and may play a role in the pathophysiology of gynecological conditions, such as endometriosis and related reproductive problems [9-12].

Decidualization, a cycle of structural and functional changes that occur within the endometrium, mainly involves differentiation of endometrial stromal cells (ESCs). Decidualization causes vigorous tissue remodeling and contributes to receptivity window for embryo implantation, maternal immune response, trophoblast invasion, establishment of placenta and fetal development [13-15]. Decidualization of ESCs is accompanied by changes in various proteins, and, cytokines, such as cyclin-D3, desmin, and trophoblastic prolactin related protein (d/tPRP) [15-17]. Decidualization of ESCs is accompanied by morphological transformation from fi-

broblastic stromal cells to enlarged, rounded, multinucleated, secretory decidual cells; a process known as mesenchymal-epithelial transition (MET). Wnt/β-catenin signaling pathway is a key signaling pathway involved in decidualization and MET [18-28]. Optimal decidualization and MET provide cyclic renewal and regeneration of endometrium, supporting embryo implantation and regulating trophoblast invasion [29-32]. Defective decidualization leads to many gynecological conditions, such as endometriosis, implantation failure and recurrent pregnancy loss [33-35].

Two recent papers in *Nature* identified that TCs express different levels of Wnts and Wnt inhibitors along the length of their intestinal crypts, where higher levels of Wnt at the base of crypts enable localized activation of Wnt signaling in stem cells [36, 37]. TCs are potentially connecting cells that directly communicate with other types of cells [38]. Previously, we demonstrated that the paracrine effect of TCs can enhance *in vitro* proliferation, adhesion, and motility of ESCs via the ERK pathway [39]. Here we hypothesize that, in uterine tissue, TCs may also interact with ESCs by releasing paracrine substances containing Wnt ligands. To confirm this, we analyzed differential expression of Wnt ligands in primary mouse ESCs and TCs. We also co-cultured TCs and ESCs to investigate *in vitro* decidualization and MET in ESCs, and the involvement of Wnt/β-catenin. We hope this study will add new evidence in the paracrine role of TCs in the pathophysiology of gynecologic conditions and decidualization insufficiency related reproductive problems.

Materials and methods

Maintenance of animals

All animal research and experimental procedures were reviewed and approved by the Ethics Committee of Soochow University (ECSU-2019000163). Specific pathogen free female BALB/C mice (25-35 g) that were of 8 to 10 weeks old were purchased from the Laboratory Animal Center of Soochow University. The animals were raised in an animal facility with constant temperature of 22°C and an ambient of photoperiod of 14 light h: 10 dark h. Female mice in estrus were mated with vigorous males of the same strain. Maintenance of vaginal plugs were recorded 0.5 days post-coitum (d p.c.).

Isolation of uterine ESCs and TCs

The uterine tissues of female BALB/c mice (3.5 d p.c.) were collected and washed 2-3 times with DMEM/F12 (Hyclone, Utah, USA) containing 100 U/mL penicillin and 0.1 mg/mL streptomycin (Beyotime, Shanghai, China). ESCs from day 4 of pregnancy were isolated and cultured as previously described [39]. Briefly, prepared uterine tissue was digested for 90 min at 4°C in 0.5% trypsin (Beyotime, Shanghai, China) to remove epithelial cells. The remaining tissue was incubated with 0.1% type-II collagenase (Sigma-Aldrich, St. Louis, MO, USA) at 37°C for 60 min. The solution was then passed through 70-μm nylon-mesh filters (BD Falcon, Heidelberg, Germany). ESCs were gathered and cultured in DMEM/F12 medium without phenol red (Hyclone, Utah, USA) containing 10% charcoal-stripped fetal bovine serum (FBS; GIBCO/Life Technologies, New York, USA) in 6-well plates at a density of 1 × 10^6/mL (Corning, New York, USA). After 4 h incubation, ESCs were grown and re-suspended in culture medium changed every other day.

Uterine TCs were also collected on day 4 of pregnancy using our previous procedures [40]. Primary TCs were seeded into 6-well plates at a density of 1 × 10^6/mL. When the TCs entered logarithmic growth phase within 3-4 days of primary cell culture, TCs were resuspended in serum-free DMEM/F12 and incubated at 37°C for 24 h. TCs-conditioned medium (TCM) was then collected and stored at -80°C.

Immunofluorescence in ESCs and TCs

Both cells populations underwent further immunofluorescence staining. First, cell samples were fixed in 4% paraformaldehyde for 15 min, washed 3 times in PBS for 5 min, and incubated with 0.5% Triton X-100 for 10 min at room temperature. After 3 washes in PBS for 5 min, ESCs and TCs were blocked with 3% bovine serum albumin (BBI, Shanghai, China) for 30 min at 37°C. Then, ESCs were incubated with rabbit anti-vimentin antibody (1:500; Cell Signaling, USA) or mouse anti-pan cytokeratin (PCK) (1:500; Cell Signaling, USA). TCs were treated with mouse anti-CD34 antibody (1:500; Abcam, USA) and rabbit anti-vimentin antibody (1:500; Abcam, USA) at 4°C overnight. Subsequently, ESCs were incubated with FITC- labeled goat anti-mouse (1:1000; MultiSciences, China) or goat anti-rabbit IgG [H+L] Dy-

Light549 (1:1000; MultiSciences, China) antibodies. TCs were incubated with Donkey anti-rabbit IgG (H+L) Alexa Fluor 488 (1:1000; Abcam, USA) or goat anti-mouse IgG (H+L) Alexa Fluor 568 (1:1000, Abcam, USA) for another 60 min at 37°C. The cells were then washed 3 times in PBS for 5 min, and then incubated with 4',6-diamidino-2-phenylindole (DAPI; Cayman; Michigan, USA.) for 5 min. Finally, samples were observed and imaged using fluorescent microscope (Nikon, Tokyo, Japan). To determine the purity of ESCs, three different fields of views were randomly selected, and the ratio of positive cells to total cells was counted.

QPCR array

A PCR array was used to determine differential mRNA expression profiles of Wnt ligands and Wnt pathway-related genes in primary TCs and ESCs. A pair of cell samples were harvested and cultured separately in vitro for 3 days. The total RNA from both samples were extracted with TRIzol (Invitrogen, CA, USA), and reversed transcribed into the first strand of cDNA as a PCR template. Then, the template was added to the reaction system (RT2 Real-Time TM SYBR Green PCR Master Mix) with TB Green™ Premix Ex Taq™ II (Tli RNaseH Plus) (Takara, Code No. RR820A), and three housekeeping gene primers in the Wnt pathway (ACTB, AES, and APC). The circulatory threshold value (Ct) of each gene in the PCR chip was calculated and data is processed according to the manufacturer's web site (http://www.wcgene.com).

Evaluating in vitro decidualization and MET

ESCs co-cultured in TCM served as the experimental group. An *in vitro* population with artificial decidualization of ESCs served as the positive control (E2-P4-cAMP). Briefly, prepared ESCs were treated with 1 μM estrogen (E2), 1 μM medroxyprogesterone 17-acetate (P4), and 0.5 mM 8-bromo-cAMP (cAMP) (all from Sigma-Aldrich) simultaneously in DMEM/F12 with 2% charcoal-treated FBS (Biological Industries Ltd, Israel) [41]. ESCs cultured in DMEM/F12 medium without phenol red was used as the blank control group. Culture medium was changed every other day, and each group of ESCs were incubated at 37°C and harvested after 3 and 5 days. Decidualization and MET were evaluated based on morphology, western blot, and RT-PCR.

Western blot

ESCs were washed with ice-cold PBS and then collected in the 1.5 mL Eppendorf tubes. Cells were then resuspended in lysis buffer (150 mmol/L NaCl, 50 mmol/L Tris-HCl, pH 7.3, and 0.25% sodium deoxycholate, 0.5% triton X-100) (Beyotime, Shanghai, China) containing 1:100 protease inhibitor cocktail (BBI, Shanghai, China) for 30 min on ice. Supernatants were collected after centrifugation. A bicinchoninic acid (BCA) reagent kit (Sangon Biotech, Shanghai, China) was used to measure protein concentration. The remaining solution was boiled in loading buffer for 10 min. The samples were run on an SDS-polyacrylamide gel. Proteins were transferred to 0.45 μm polyvinylidene fluoride (PVDF; Millipore, MA, USA) membranes. The membranes were blocked in 5% non-fat milk powder in 0.5% in tris-buffered saline with Tween-20 (TBST; Sangon Biotech, Shanghai, China) for 90 min. Membranes were incubated in primary antibodies diluted in TBST at 4°C overnight and then washed 3 times in TBST for 5 min. Membranes were further incubated in secondary antibodies for 60 min and detected with chemiluminescent HRP substrate diluted in TBST. Primary antibodies used were cyclin-D3, desmin, E-cadherin, N-cadherin, β-catenin, FOXO1, and β-tubulin (1:1000, Cell Signaling Technologies, MA, USA). The anti-mouse or anti-rabbit secondary antibodies were detected with chemiluminescent HRP substrate (1:5000, Absin Bioscience Inc., Shanghai, China). A gel imaging system was used to obtain images of membranes.

Quantitative real-time PCR

ESCs and TCs were harvested in Eppendorf tubes and lysed using TRIzol (Invitrogen, CA, USA) according to the manufacturer's protocol. Then 1 μg of total cellular RNA was reverse-transcribed to cDNA with Reverse Transcriptase M-MLV (RNase H-) (TaKaRa, Japan) to a final volume of 10 μL. Then, 1 μL of cDNA was added into TB Green® Premix Ex Taq™ (Tli RNaseH Plus) (TaKaRa, Japan) to final volume of 20 μL. Quantitative real-time PCR was performed using ABI QuantStudio3 Detection System (Applied Biosystems, Carlsbad, CA). Relative expression of the samples was measured using the ΔΔCT method. Each sample was run in triplicate. The house-keeping gene GAPDH was

Table 1. List of qRT-PCR primers

Gene	Forward	Reverse
E-cadherin	CAGTTCCGAGGTCTACACCTT	TGAATCGGGAGTCTTCCGAAAA
N-cadherin	AGGCTTCTGGTGAAATTGCAT	GTCCACCTTGAAATCTGCTGG
Cyclin D3	TGCGTGCAAAAGGAGATCAAG	GGACAGGTAGCGATCCAGGT
d/tPRP	TTATGGGTGCATGGATCACTCC	CCCACGTAAGGTCATCATGGAT
CTNNB1	ATGGAGCCGGACAGAAAAGC	TGGGAGGTGTCAACATCTTCTT
FOXO1	CCCAGGCCGGAGTTTAACC	GTTGCTCATAAAGTCGGTGCT
GAPDH	AGGTCGGTGTGAACGGATTTG	GGGGTCGTTGATGGCAACA

used to normalize individual samples. A list of primer sequences is provided in **Table 1**.

Plasmid construction and transfection in ESCs

β-catenin knockdown in ESCs was performed to validate that mechanisms involved in TCs altered of ESCs. Two pairs of 58 bp oligonucleotides (shRNA1 and shRNA2) encoding a 21 bp shRNA were designed to silence the mouse CTNNB1 gene to knockdown β-catenin in ESCs. A scramble shRNA was also used as a control. shRNA sequences that targeted mouse β-catenin are shown in **Table 2** with interfering sequences acquired from Sigma (www.sigmaaldrich.com). Expressed sequence tags (EST) were analyzed using the basic local alignment search tool (BLAST) from the National Center for Biotechnology Information (NCBI) to verify that the shRNA only targeted mouse CTNNB1. Two pairs of shRNA encoded nucleotides were designed to target various parts of CTNNB1 mRNA and were synthesized by GENEWIZ, Inc (www.genewiz.com.cn). Equal volumes of sense and antisens oligonucleotides were mixed and heated at 94°C for 4 min, then cooled in 5 min increments at 70°C, 60°C, 50°C, 40°C, and 20°C for 5 min. The annealed oligonucleotides were inserted into a PLKO.1-GFP vector (a kind gift from Professor Jian-Hong Chu, at the Institute of Blood and Marrow Transplantation, Suzhou City, China) using T4 DNA ligase (NEB, New England Biolabs, MA, USA). The PLKO.1-GFP vector was digested with EcoRI (NEB, New England Biolabs, MA, USA) and AgeI (New England Biolabs, MA, USA). Recombinant vectors were validated by sequencing (GENEWIZ, NJ, USA). The envelope plasmid (pMD2.G) and packaging plasmid (psPAX2) were co-transfected with recombinant plasmid into 293T cells for lentivirus production.

Lentivirus from 293T cell supernatants were harvested 3 days after transfection. Primary ESCs were transduced with plasmid lentiviruses (sh-scramble, sh1-β-catenin, sh2-β-catenin) for 24 h, followed by exposure to TCM for another 3 days. Experimental groups are referred to as "shRNA1 + TCM" and "shRNA2 + TCM". The negative control group is referred to as "sh-scramble + TCM". And the blank control (BC) is referred to as "DMEM/F12 + TCM".

Statistical analysis

Protein and mRNA samples were prepared from at least two independent primary cell cultures subjected to identical experimental procedures. Differences among control and experimental groups were analyzed by one-way analysis of variance, followed by Tukey post hoc test using GraphPad Prism 8.0 (GraphPad Software, CA). Data are presented as mean ± standard deviation (SD). A P value of < 0.05 was considered to be statistically significant, and is presented as $*P < 0.05$, $**P < 0.01$, or $***P < 0.001$.

Results

Identifying ESCs and TCs

Primary ESCs were successfully isolated (96.2% ± 2.5% of population) showing typical morphology: fusiform, clear outline, and sparse intercellular links. Immunofluorescence showed positive vimentin staining and negative cytokeratin staining (**Figure 1A-F**).

Primary uterine TCs were successfully isolated showing typical morphology: irregular cell body shape with long Tps extension that branch from the cell body (**Figure 2A**). Characteristic Tps displayed alternating thin podomers and thick podoms segments. TCs were double-positive for vimentin/CD34 staining (**Figure 2B-D**), consistent with our previous research [39].

Differential expression of Wnt pathway mRNA in TCs and ESCs

Relative expression of 85 Wnt ligands and pathway related genes in TCs and ESCs were determined by a qPCR array (**Figure 3**). TCs had high expression of Wnt ligands and pathway genes compared to ESCs. High expression of the following genes were observed: *FZD4,*

Table 2. shRNA sequences targeted mouse β-catenin

shRNA1	5-CCGGGCTGATATTGACGGGCAGTATCTCGAGATACTGCCCGTCAATATCAGCTTTTTG-3
	3-AATTCAAAAAGCTGATATTGACGGGCAGTATCTCGAGATACTGCCCGTCAATATCAGC-5
shRNA2	5-CCGGCCCAAGCCTTAGTAAACATAACTCGAGTTATGTTTACTAAGGCTTGGGTTTTTG-3
	3-AATTCAAAAACCCAAGCCTTAGTAAACATAACTCGAGTTATGTTTACTAAGGCTTGGG-5
Scramble	5-CCGGCGAGTAGAGACTGATCAACATCTCGAGATGTTGATCAGTCTCTACTCGTTTTTG-3
	3-AATTCAAAAACGAGTAGAGACTGATCAACATCTCGAGATGTTGATCAGTCTCTACTCG-5

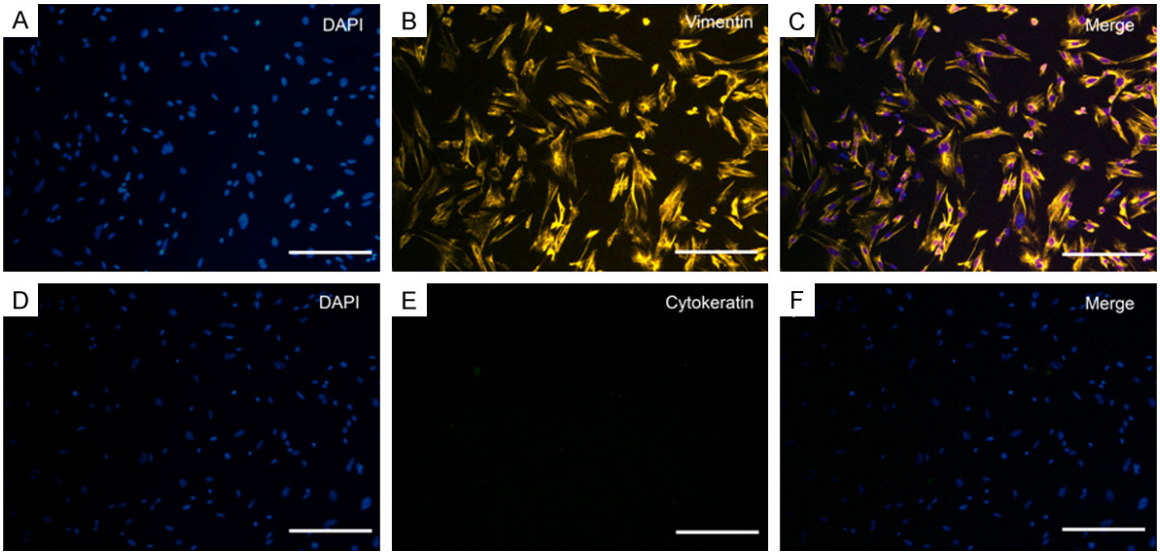

Figure 1. Typical morphological and immune profiles of uterine ESCs from mice. Immunofluorescence staining in ESCs was positive for vimentin (A-C) and negative for cytokeratin (D-F). Three fields of views were randomly selected under the microscope, and the ratio of positive cells to total cells was counted. The purity of the ESCs population was 96.2% ± 2.5%. Scale bar = 50 μm.

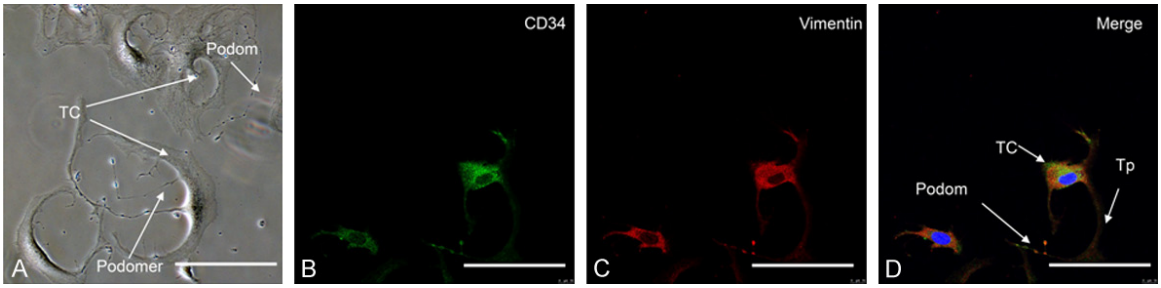

Figure 2. Typical morphological and immune profiles of uterine TCs from mice uterus. A. Phase-contrast limages showed TCs had irregular cell body shapes and characteristic Tps extending from the cell body, with typical alternating podoms (thick segment) and podomers (thin segment). B. CD34 labeled with Alexa Fluor 488 (green). C. Vimentin labeled with (red). D. Merged image showing co-expression of CD34 and vimentin in the whole length of TCs. Representative TCs are shown with, small cell bodies with long Tps, characterized by moniliform outline and alternating podom and podomers. Nuclei were counterstained with DAPI (blue). Scale bar = 50 μm.

WIF1, SFRP4, SFRP1, FZD8, CCND1, WNT4, WNT2, TCF711, LRP5, SFRP2, NFATC1, DKK1, CTNNB1, CTNNBIP1, AES, RUVBL1, FZD1, KREMEN1, CCND2, DVL2, FOS11, FRZB, and *FZD9*. Low expression of the follow genes were observed: *WNT9A, WNT16, TCF7, WNT5A, FZD6, AXIN2, LEF1, MYC, NLK, WISP1, FOXN1,* and *SOX17* (**Figure 3B**).

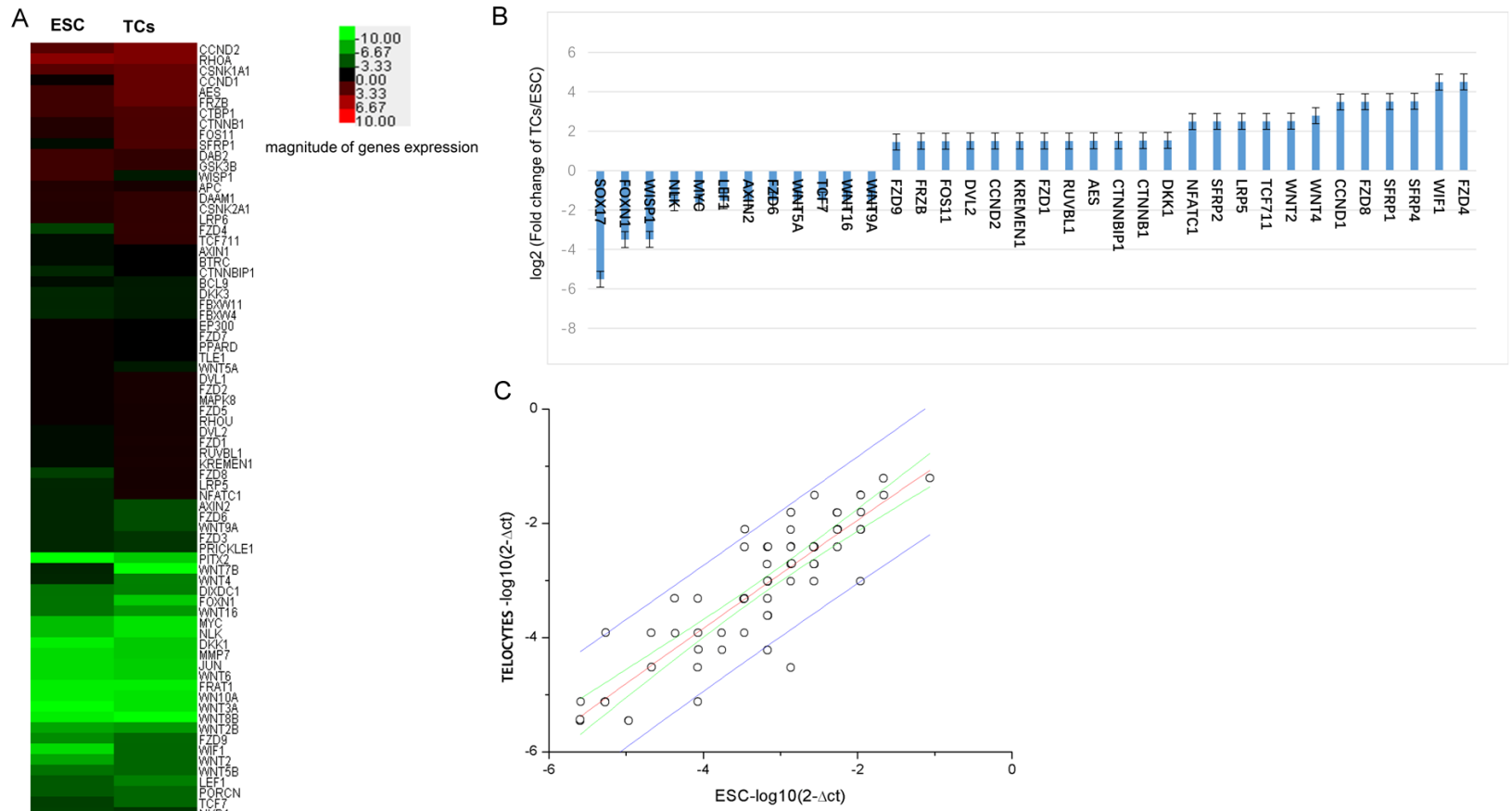

Figure 3. Differential mRNA expression profiles of Wnt ligands and Wnt pathway related genes in primary TCs and primary ESCs. A. Heat map relative expression of a 85 mRNAs in (TCs and ESCs) red = high; green = low. B. Histogram showing relatively high or low expression of Wnt ligands and pathway related genes. Changes in levels shown using log2 scale. C. Scatter plots showing differences in gene expression between TCs and ESCs. Values plotted on the X and Y axes represent mean normalized signal values for each group using a log2 scale.

TCM induced decidualization, MET and β-catenin activation in ESCs

Samples from the blank control and experimental group were collected on day 3 and 5. The impact of TCM on ESCs were time-dependent. Decidualization related proteins (cyclin-D3 and desmin), an epithelial cell marker of MET (E-cadherin), and β-catenin related proteins (β-catenin, FOXO1) in experimental ESCs tended to increase between day 3 and 5. In contrast, a stromal cell marker of MET (N-cadherin) tended to decrease (**Figure 4A**).

The three groups of ESCs were incubated for 3 days for further observation. Morphology changes of ESCs are shown in (**Figure 4I-K**). In the blank control without any exogenous stimulus, ESCs had typical stromal cell morphology: scattered with a clearly defined slender spindle shape, and no obvious intercellular linkage (**Figure 4I**). After TCM exposure, ESCs gradually transformed towards epithelial cell phenotypes: multinuclear round cells with secretory, translucent and abundant cytoplasm, and some spindle-like cells that were tightly linked together (**Figure 4J**). In the positive control group, ESCs were tightly linked to each other, transforming from spindle shaped which resembled stromal cells, to round shaped, which resembled epithelial cells (**Figure 4K**).

Western blots showed increased expression-cyclin-D3 and desmin, and RT-PCR showed increased cyclin D3 and d/tPRP mRNA in experimental ESCs compared to the blank control, while lower than the positive control. There were still significant differences ($P < 0.05$, one-way ANOVA) among the three groups for each marker (**Figure 4D**, **4E** and **4H**). Therefore, TCM induced a significant effect on ESC decidualization, but less than the positive control.

Elevated E-cadherin mRNA and protein was identified by RT-PCR and western blot, respectively, elevated in experimental ESCs compared to the blank control. In contrast, N-cadherin mRNA and protein decreased. E-cadherin was lower and N-cadherin was higher compared to the positive control (**Figure 4B** and **4H**). However, mRNA levels were significantly different ($P < 0.05$, one-way ANOVA) between three groups for each marker (**Figure 4C** and **4H**). Therefore, accompanied by decidualization, TCM also induced significant MET in ESCs, but weaker than the positive control.

Changes to Wnt/β-catenin signaling pathways in ESCs were further investigated. β-catenin and downstream *FOXO1* expression were increased after TCM exposure (**Figure 4H**). RT-PCR also showed similar trends in *CTNNB1, FOXO1* expression, with significant differences ($P < 0.05$, one-way ANOVA) in mRNA levels between the three groups (**Figure 4F** and **4G**). Therefore, through activation of β-catenin and its downstream transcription factor FOXO1, TCM induced *in vitro* decidualization of ESCs and MET.

Knockdown of β-catenin in ESCs

ESCs was transduced with shRNA targeting β-catenin for 24 h, and then co-cultured with TCM for another 3 days to efficiently decrease transcription and expression of *CTNNB1*. Expression of β-catenin was decreased (**Figure 5A**), with significantly decreased levels of *CTNNB1* mRNA (**Figure 5B**), compared to the negative control. Thus, shRNA-mediated repression of β-catenin gene expression was successfully confirmed in ESCs.

Knockdown of β-catenin altered the morphology of ESCs, to round/elliptical shapes, epithelial cell features of decidual cells in the negative control (**Figure 5C**), and to spindle-shaped stromal cells in experimental ESCs (**Figure 5D**, **5E**). Meanwhile, downregulation of β-catenin via shRNA1 and shRNA2 in ESCs showed decreased expression of cyclin-D3, desmin, E-cadherin, and FOXO1, but increased N-cadherin compared to two control samples determined by western blot (**Figure 5K**) or RT-PCR ($P < 0.05$, one-way ANOVA) (**Figure 5F-J**). Proteins expression remained unchanged between the two control samples (**Figure 5K**). Therefore, β-catenin knockdown prevented or reversed TCM-induced decidualization and MET in ESCs.

Discussion

TCs have been identified in female reproductive system, interacting with various surrounding cells with Tps, and release paracrine exosomes and/or vesicles to regulate nearby and distant target cells. Therefore, TCs play a potential role in pathophysiology in obstetric and gynecological conditions, such as uterine, endometrium, placenta and pregnancy related diseases [10]. Uterine TCs express estrogen and progesterone receptors, with cell morphology and populations dependent on different

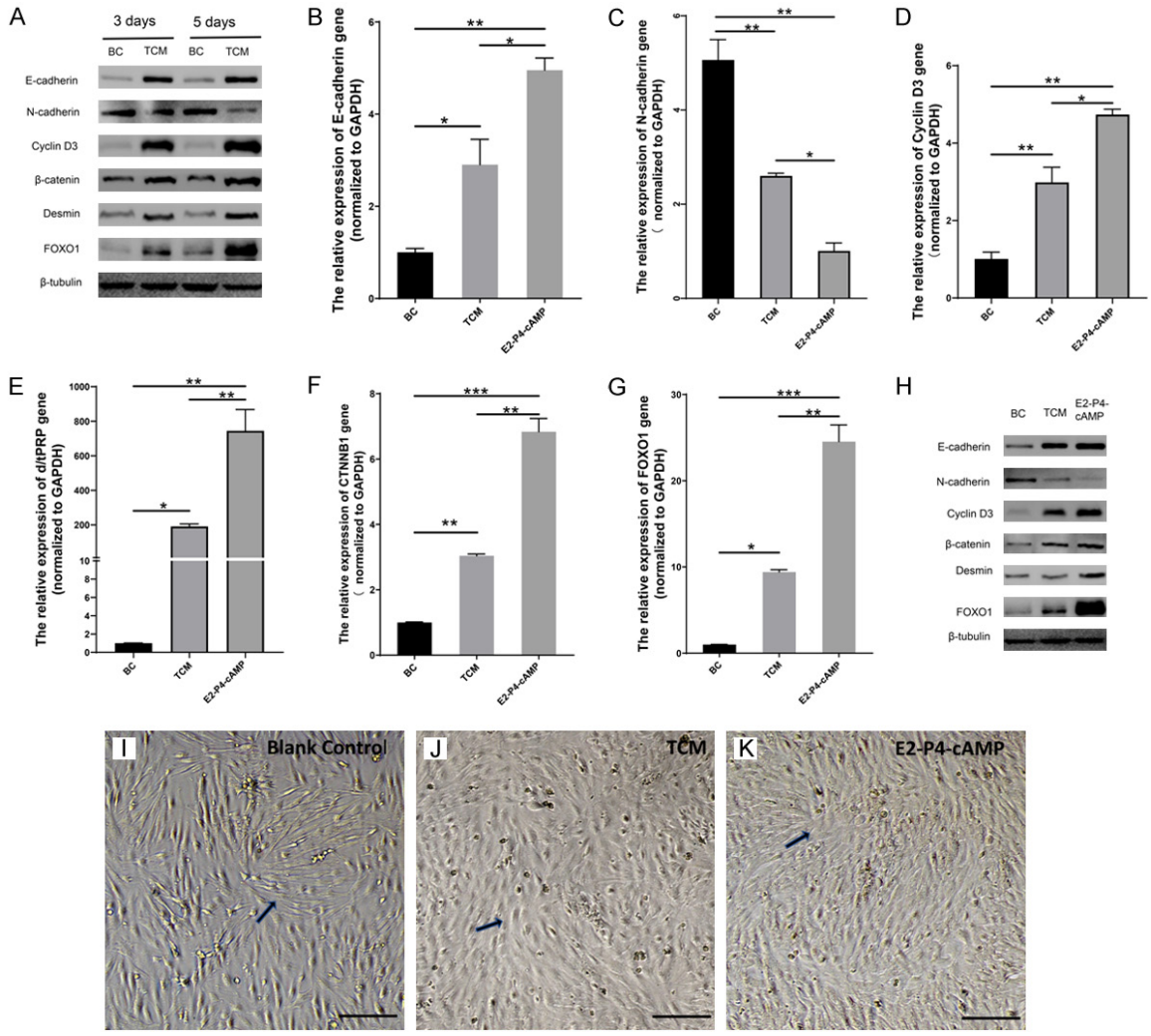

Figure 4. TCM enhanced decidualization and MET in ESCs via activating the Wnt/β-catenin signaling pathway. (A) Western blot analysis showed that cyclin-D3, desmin, E-cadherin, β-catenin and FOXO1 in experimental ESCs increased between samples collected on day 3 and day 5, N-cadherin levels decreased compared to the blank control (BC). Therefore, TCM-induced alterations in ESCs were time-dependent. (B-G) RT-PCR analysis of mRNA expression showed significant differences between three groups (BC, TCM, E2-P4-cAMP) for each marker. Relative mRNA expression was determined by normalizing to GAPDH levels. Error bars show SD from two independent experiments where, $*P < 0.05$, $**P < 0.01$, or $***P < 0.001$ by one-way ANOVA with Tukey post hoc test. (H) Western blot analysis showed increased cyclin-D3, desmin, E-cadherin, β-catenin, and FOXO1 on 3 day. Additionally, levels of stromal cell marker (N-cadherin) decreased in experimental ESCs (TCM) compared to the blank control (BC). Cyclin-D3, Desmin E-cadherin, β-catenin, and FOXO1 levels were lower and N-cadherin levels were higher than the positive control (E2-P4-cAMP). Results were from three independent experiments and β-tubulin was used as the loading control. Images of ESCs using phase-contrast microscopy. (I) For the BC group, ESCs were spindle-shaped, clearly defined, and scattered without any obvious intercellular linkage. (J) After TCM treatment, ESCs gradually became round with some spindle-like cells that were tightly linked together. (K) While in E2-P4-cAMP, ESCs had an oval multinucleated appearance and were tightly linked. Thus, the transition of ESCs from spindle shape morphology to round stromal cells is reflective of experimental conditions. Representative cells are denoted by black arrows. Scale bar = 50 μm.

gestational ages, thus, TCs were predicted to be involved in physiologyical changes that occur during pregnancy [42]. Uterine TCs also express connexin 43, a gap junction protein, and may be involved in decidual maturation of endometrium [43]. Previously, our group described immunoregulatory roles for uterine TCs *in vitro*, by activating and maintaining the immune response of peritoneal macrophages through paracrine signaling [44], and direct

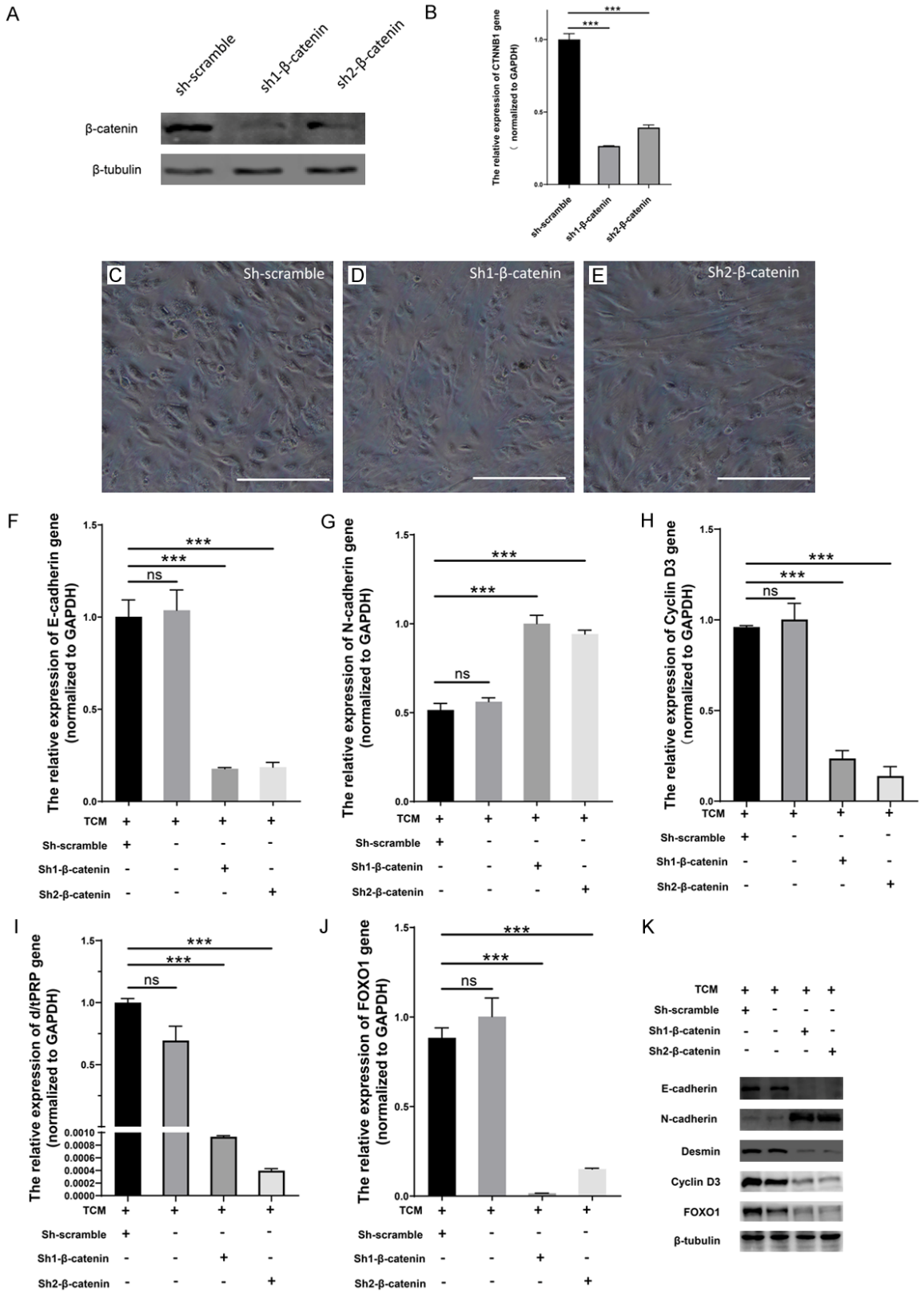

Figure 5. β-catenin knockdown blocked or reversed TCM-induced decidualization and MET in ESCs. A. Supernatant of plasmid lentiviruses, sh-scramble, sh1-β-catenin, sh2-β-catenin, were used to transfect ESCs. Western blot analysis showed decreased expression of β-catenin. B. *CTNNB1* mRNA levels were significantly reduced in experimental conditions (sh1-β-catenin, sh2-β-catenin), compared with negative control (sh-scramble) by RT-PCR analysis. Error

bars indicate SD from two independent experiments where *P < 0.05, **P < 0.01, or ***P < 0.001 by one-way ANOVA with Tukey post hoc test. β-catenin knockdown showed morphological changes and ESC transition using phase-contrast microscopy. C. Round or elliptical shapes were representative features of negative control decidual cells treated with sh-scramble. D, E. Stromal cells, with spindle-shapes, clear outlines, and sparse intercellular linkages were observed in β-catenin-shRNA treated ESCs (sh1-β-catenin, sh2-β-catenin). Scale bar = 50 μm. F-J. mRNA expression was analyzed by RT-PCR in four groups of ESCs (TCM, sh-scream, sh1-β-catenin, sh2-β-catenin). Relative mRNA expression was determined by normalizing to GAPDH levels. Error bars show SD from two independent experiments, where ns = non-significant, *P < 0.05, **P < 0.01, or ***P < 0.001 by ANOVA with Tukey post hoc test. K. Western blot analysis showed that β-catenin downregulation via shRNA1 and shRNA2 treatment in ESCs decreased expression cyclin-D3, desmin, E-cadherin, and FOXO1. Increased expression of N-cadherin was also observed compared to two controls. β-tubulin levels remained unchanged and used as the loading control.

cell-to-cell interaction via mitochondrial signaling [40]. Further, paracrine substances from TCs enhanced ESCs activity via the ERK-cyclin-D3 signaling pathway, thus, affecting endometrium related diseases [39]. Recent studies show that stromal cells and TCs are elusive Wnt-producing niche cells, forming subepithelial networks to support Wnt family ligands and related proteins and renewal of adjacent cells and tissue in intestinal crypts [36, 37, 45, 46]. Additionally, TCs transplantation can attenuate unilateral ureter obstruction-induced renal fibrosis by enhanced MET in rat kidney tissue [47]. A therapeutic role of TCs has also been shown in ovalbumin-induced acute asthma in mice [48]. In this study, we found that, by releasing paracrine substances containing Wnt family ligands, uterine TCs can enhance in vitro decidualization and MET in ESCs, which were mediated by the Wnt/β-catenin pathway. This may be critical for managing defective decidualization in endometrium.

Wnt subtypes include Wnt4, Wnt5a, Wnt7a, Wnt7b, Wnt11, Wnt16, Fzd2, Fzd4, and Fzd6, which are all up-regulated in the uterus during embryo implantation. Wnt4 is the most abundant in decidual endometrium, playing a key role in regulating ESCs decidualization and embryo implantation. Wnt7a, Wnt7b, and Wnt11 are abundantly expressed in endometrial glandular epithelium [18, 28, 49]. A wide range of signaling molecules, including Wnt/β-catenin, are involved in ESCs decidualization. β-catenin is the central player in canonical Wnt signaling, and is activated after extracellular Wnt ligands stimulation, facilitating endometrial decidualization [21, 50]. Depletion of Wnt4 and β-catenin decreases decidual response and impairs fertility capacity in female mice [25, 28]. FOXO1 is controlled by upstream activation of β-catenin and then interact with PGR or CCAAT/enhancer binding protein, playing an essential role in regulating differentiation and decidualization in ESCs. Knockdown of FOXO1 can inhibit decidualization of ESCs [50-52]. In this study, TCs showed higher Wnt expression ratio than ESCs (**Figure 3**). Wnts are secreted proteins that bind to target cell-surface receptors to activate the Wnt/β-catenin signaling pathway [53]. Release of these paracrine substances from TCs, especially Wnt4, may explain the observed decidualization, MET and underlying β-catenin activation in ESCs.

Decidual ESCs can create paracrine gradients essential for uterine receptivity and support for post-implantation pregnancy [54]. Proper endometrium decidualization is critical for embryo selection, implantation, and trophoblast development. Defective ESCs decidualization has recently been highlighted as an underlying cause of endometriosis, recurrent implantation failure, miscarriage, and preeclampsia [55-58]. MET is natural physiological process that accompanies ESCs decidualization. During MET, mesenchymal cells lose their movement and migration characteristics, obtain cell polarity, and change its morphology from spindle-shaped to polarized adherent epithelial cells [59]. Downregulation of mesenchymal components, vimentin, fibronectin, and N-cadherin, is coupled with upregulation of epithelial cell adhesion molecules, such as E-cadherin. Epithelial-mesenchymal transition (EMT) is the reversed process of MET, and Wnt/β-catenin is also key pathway involved in this process [60]. The dynamic balance of MET/EMT is essential for endometrial regeneration and differentiation, and preparation for embryo implantation and development [29, 30]. Failure of MET will inevitably lead to pregnancy loss.

This study demonstrated that TCM-induced decidualization and MET in ESCs via activating Wnt/β-catenin signaling by reporting, several changes in morphology and secretory markers. Knockdown of *CTNNB1* blocked β-catenin sig-

naling in ESCs, decreasing decidualization and MET in ESCs. ERK pathway activation by Wnt signaling can also occur at multiple levels [61]. Previously observed TCM-induced ERK activation in ESCs may have also resulted from β-catenin-independent signaling [39]. Thus, TCs may be central signaling coordination hubs in uterine tissues, and both Wnt/β-catenin and ERK pathways may be involved in TCs induced activation of ESCs.

Conclusion

Consistent with recent reports of Wnts activation in stromal cells in intestinal maintenance [36, 37, 45, 46], our results confirmed that, by releasing paracrine substances, TCs induced decidualization and MET in ESCs, via activation of Wnt/β-catenin signaling. This study provided new evidence for paracrine signaling of TCs, and offers new insights into mechanisms of normal endometrium renewal and regeneration. Using TCs or the combination of TCs and ESCs is a promising way to treat defective decidualization and improve endometrial receptivity in gynecological conditions and reproductive disorders.

Acknowledgements

The authors thank Professor Jian-Hong Chu, Institute of Blood and Marrow Transplantation, Suzhou, China, for the PLKO.1-GFP vector he provided friendly. The authors also thank the National Natural Science Foundation of China (81971335 and 81571415 to X-J.Y.), which supported this study.

Disclosure of conflict of interest

None.

Abbreviations

ESCs, endometrial stromal cells; TCs, Telocytes; MET, mesenchymal-epithelial transition; d/tPRP, trophoblastic prolactin related protein; Tps, telopodes; EMT, epithelial-mesenchymal transition; d p.c., days post coitum; DAPI, 4',6-diamidino-2-phenylindole; FBS, fetal bovine serum.

Address correspondence to: Xiao-Jun Yang, Department of Obstetrics and Gynecology, The First Affiliated Hospital of Soochow University, 188 Shizi Road, Suzhou 215006, Jiangsu Province, PR China. Tel: +86-186-2629-2163; Fax: +86-512-66919883; E-mail: yang.xiaojun@hotmail.com

References

[1] Faussone Pellegrini MS and Popescu LM. Telocytes. Biomol Concepts 2011; 2: 481-489.
[2] Cretoiu SM and Popescu LM. Telocytes revisited. Biomol Concepts 2014; 5: 353-369.
[3] Yang J, Li Y, Xue F, Liu W and Zhang S. Exosomes derived from cardiac telocytes exert positive effects on endothelial cells. Am J Transl Res 2017; 9: 5375.
[4] Cismasiu VB and Popescu LM. Telocytes transfer extracellular vesicles loaded with microRNAs to stem cells. J Cell Mol Med 2015; 19: 351-358.
[5] Albulescu R, Tanase C, Codrici E, Popescu DI, Cretoiu SM and Popescu LM. The secretome of myocardial telocytes modulates the activity of cardiac stem cells. J Cell Mol Med 2015; 19: 1783-1794.
[6] Qi G, Lin M, Xu M, Manole CG, Wang X and Zhu T. Telocytes in the human kidney cortex. J Cell Mol Med 2012; 16: 3116-3122.
[7] Bei Y, Wang F, Yang C and Xiao J. Telocytes in regenerative medicine. J Cell Mol Med 2015; 19: 1441-1454.
[8] Bojin FM, Gavriliuc OI, Cristea MI, Tanasie G, Tatu CS, Panaitescu C and Paunescu V. Telocytes within human skeletal muscle stem cell niche. J Cell Mol Med 2011; 15: 2269-2272.
[9] Roatesi I, Radu BM, Cretoiu D and Cretoiu SM. Uterine telocytes: a review of current knowledge. Biol Reprod 2015; 93: 10.
[10] Aleksandrovych V, Walocha JA and Gil K. Telocytes in female reproductive system (human and animal). J Cell Mol Med 2016; 20: 994-1000.
[11] Nizyaeva NV, Sukhacheva TV, Serov RA, Kulikova GV, Nagovitsyna MN, Kan NE, Tyutyunnik VL, Pavlovich SV, Poltavtseva RA and Yarotskaya EL. Ultrastructural and immunohistochemical features of telocytes in placental villi in preeclampsia. Sci Rep 2018; 8: 3453.
[12] Janas P, Kucybala I, Radon-Pokracka M and Huras H. Telocytes in the female reproductive system: an overview of up-to-date knowledge. Adv Clin Exp Med 2018; 27: 559-565.
[13] Dunn CL, Kelly RW and Critchley HO. Decidualization of the human endometrial stromal cell: an enigmatic transformation. Reprod Biomed Online 2003; 7: 151-161.
[14] Ramathal CY, Bagchi IC, Taylor RN and Bagchi MK. Endometrial decidualization: of mice and men. Semin Reprod Med 2010; 28: 17-26.
[15] Matsumoto K, Yamauchi N, Watanabe R, Oozono S, Kubota K, Nishimura K, Wood C,

Soh T, Kizaki KI and Hattori MA. In vitro decidualization of rat endometrial stromal cells. Cell Tissue Res 2009; 335: 575-583.
[16] Zhang P, Tang M, Zhong T, Lin Y, Zong T, Zhong C, Zhang B, Ren M and Kuang H. Expression and function of kisspeptin during mouse decidualization. PLoS One 2014; 9: e97647.
[17] Sroga JM, Ma X, Gao F and Das SK. Replaceable cyclin D3 (CycD3) improves decidualization (Dcz) defects in HOXA-10-/- mice. Fertil Steril 2012; 98: S23-S24.
[18] Hayashi K, Erikson DW, Tilford SA, Bany BM, Maclean JA 2nd, Rucker EB 3rd, Johnson GA and Spencer TE. Wnt genes in the mouse uterus: potential regulation of implantation. Biol Reprod 2009; 80: 989-1000.
[19] Li Q, Kannan A, Wang W, Demayo FJ, Taylor RN, Bagchi MK and Bagchi IC. Bone morphogenetic protein 2 functions via a conserved signaling pathway involving Wnt4 to regulate uterine decidualization in the mouse and the human. J Biol Chem 2007; 282: 31725-31732.
[20] Miller C and Sassoon DA. Wnt-7a maintains appropriate uterine patterning during the development of the mouse female reproductive tract. Development 1998; 125: 3201-3211.
[21] Sonderegger S, Pollheimer J and Knofler M. Wnt signalling in implantation, decidualisation and placental differentiation--review. Placenta 2010; 31: 839-847.
[22] Wang Q, Lu J, Zhang S, Wang S, Wang W, Wang B, Wang F, Chen Q, Duan E, Leitges M, Kispert A and Wang H. Wnt6 is essential for stromal cell proliferation during decidualization in mice. Biol Reprod 2013; 88: 5.
[23] Chen Q, Zhang Y, Lu J, Wang Q, Wang S, Cao Y, Wang H and Duan E. Embryo-uterine cross-talk during implantation: the role of Wnt signaling. Mol Hum Reprod 2009; 15: 215-221.
[24] Hess AP, Hamilton AE, Talbi S, Dosiou C, Nyegaard M, Nayak N, Genbecev-Krtolica O, Mavrogianis P, Ferrer K, Kruessel J, Fazleabas AT, Fisher SJ and Giudice LC. Decidual stromal cell response to paracrine signals from the trophoblast: amplification of immune and angiogenic modulators. Biol Reprod 2007; 76: 102-117.
[25] Jeong JW, Lee HS, Franco HL, Broaddus RR, Taketo MM, Tsai SY, Lydon JP and DeMayo FJ. beta-catenin mediates glandular formation and dysregulation of beta-catenin induces hyperplasia formation in the murine uterus. Oncogene 2009; 28: 31-40.
[26] Xie H, Tranguch S, Jia X, Zhang H, Das SK, Dey SK, Kuo CJ and Wang H. Inactivation of nuclear Wnt-beta-catenin signaling limits blastocyst competency for implantation. Development 2008; 135: 717-727.
[27] Mohamed OA, Jonnaert M, Labelle-Dumais C, Kuroda K, Clarke HJ and Dufort D. Uterine Wnt/β-catenin signaling is required for implantation. Proc Natl Acad Sci U S A 2005; 102: 8579-8584.
[28] Franco HL, Dai D, Lee KY, Rubel CA, Roop D, Boerboom D, Jeong JW, Lydon JP, Bagchi IC, Bagchi MK and DeMayo FJ. WNT4 is a key regulator of normal postnatal uterine development and progesterone signaling during embryo implantation and decidualization in the mouse. FASEB J 2011; 25: 1176-1187.
[29] Zhang XH, Liang X, Liang XH, Wang TS, Qi QR, Deng WB, Sha AG and Yang ZM. The mesenchymal-epithelial transition during in vitro decidualization. Reprod Sci 2013; 20: 354-360.
[30] Patterson AL, Zhang L, Arango NA, Teixeira J and Pru JK. Mesenchymal-to-epithelial transition contributes to endometrial regeneration following natural and artificial decidualization. Stem Cells Dev 2013; 22: 964-974.
[31] Zhang L, Patterson AL, Zhang L, Teixeira JM and Pru JK. Endometrial stromal beta-catenin is required for steroid-dependent mesenchymal-epithelial cross talk and decidualization. Reprod Biol Endocrinol 2012; 10: 75.
[32] Godbole G, Suman P, Gupta SK and Modi D. Decidualized endometrial stromal cell derived factors promote trophoblast invasion. Fertil Steril 2011; 95: 1278-1283.
[33] Klemmt PA, Carver JG, Kennedy SH, Koninckx PR and Mardon HJ. Stromal cells from endometriotic lesions and endometrium from women with endometriosis have reduced decidualization capacity. Fertil Steril 2006; 85: 564-572.
[34] Su RW, Strug MR, Joshi NR, Jeong JW, Miele L, Lessey BA, Young SL and Fazleabas AT. Decreased Notch pathway signaling in the endometrium of women with endometriosis impairs decidualization. J Clin Endocrinol Metab 2015; 100: E433-442.
[35] Salker M, Teklenburg G, Molokhia M, Lavery S, Trew G, Aojanepong T, Mardon HJ, Lokugamage AU, Rai R, Landles C, Roelen BA, Quenby S, Kuijk EW, Kavelaars A, Heijnen CJ, Regan L, Macklon NS and Brosens JJ. Natural selection of human embryos: impaired decidualization of endometrium disables embryo-maternal interactions and causes recurrent pregnancy loss. PLoS One 2010; 5: e10287.
[36] Degirmenci B, Valenta T, Dimitrieva S, Hausmann G and Basler K. GLI1-expressing mesenchymal cells form the essential Wnt-secreting niche for colon stem cells. Nature 2018; 558: 449-453.
[37] Shoshkes-Carmel M, Wang YJ, Wangensteen KJ, Toth B, Kondo A, Massasa EE, Itzkovitz S and Kaestner KH. Subepithelial telocytes are an important source of Wnts that supports intestinal crypts. Nature 2018; 557: 242-246.
[38] Song D, Yang D, Powell CA and Wang X. Cell-cell communication: old mystery and new opportunity. Cell Biol Toxicol 2019; 35: 89-93.

[39] Tang XL, Zhang FL, Jiang XJ and Yang XJ. Telocytes enhanced the proliferation, adhesion and motility of endometrial stromal cells as mediated by the ERK pathway in vitro. Am J Transl Res 2019; 11: 572.
[40] Jiang XJ, Cretoiu D, Shen ZJ and Yang XJ. An in vitro investigation of telocytes-educated macrophages: morphology, heterocellular junctions, apoptosis and invasion analysis. J Transl Med 2018; 16: 85.
[41] Kommagani R, Szwarc MM, Kovanci E, Gibbons WE, Putluri N, Maity S, Creighton CJ, Sreekumar A, DeMayo FJ, Lydon JP and O'Malley BW. Acceleration of the glycolytic flux by steroid receptor coactivator-2 is essential for endometrial decidualization. PLoS Genet 2013; 9: e1003900.
[42] Banciu A, Banciu D, Mustaciosu C, Radu M, Cretoiu D, Xiao J, Cretoiu S, Suciu N and Radu B. Beta-estradiol regulates voltage-gated calcium channels and estrogen receptors in telocytes from human myometrium. Int J Mol Sci 2018; 19: 1413.
[43] Ye TM, Pang RT, Leung CO, Liu W and Yeung WS. Development and characterization of an endometrial tissue culture model for study of early implantation events. Fertil Steril 2012; 98: 1581-1589.
[44] Chi C, Jiang XJ, Su L, Shen ZJ and Yang XJ. In vitro morphology, viability and cytokine secretion of uterine telocyte-activated mouse peritoneal macrophages. J Cell Mol Med 2015; 19: 2741-2750.
[45] Greicius G, Kabiri Z, Sigmundsson K, Liang C, Bunte R, Singh MK and Virshup DM. PDGFRalpha(+) pericryptal stromal cells are the critical source of Wnts and RSPO3 for murine intestinal stem cells in vivo. Proc Natl Acad Sci U S A 2018; 115: E3173-E3181.
[46] Kabiri Z, Greicius G, Madan B, Biechele S, Zhong Z, Zaribafzadeh H, Aliyev J, Wu Y, Bunte R and Williams BO. Stroma provides an intestinal stem cell niche in the absence of epithelial Wnts. Development 2014; 141: 2206-2215.
[47] Zheng L, Li L, Qi G, Hu M, Hu C, Wang S, Li J, Zhang M, Zhang W, Zeng Y, Zhang Y, Li L, Wang X, Lin M, Zhu T and Rong R. Transplantation of telocytes attenuates unilateral ureter obstruction-induced renal fibrosis in rats. Cell Physiol Biochem 2018; 46: 2056-2071.
[48] Ye L, Song D, Jin M and Wang X. Therapeutic roles of telocytes in OVA-induced acute asthma in mice. J Cell Mol Med 2017; 21: 2863-2871.
[49] Cheng CW, Smith SK and Charnock-Jones DS. Transcript profile and localization of Wnt signaling-related molecules in human endometrium. Fertil Steril 2008; 90: 201-204.
[50] Li Q, Kannan A, Das A, Demayo FJ, Hornsby PJ, Young SL, Taylor RN, Bagchi MK and Bagchi IC. WNT4 acts downstream of BMP2 and functions via beta-catenin signaling pathway to regulate human endometrial stromal cell differentiation. Endocrinology 2013; 154: 446-457.
[51] Buzzio OL, Lu Z, Miller CD, Unterman TG and Kim JJ. FOXO1A differentially regulates genes of decidualization. Endocrinology 2006; 147: 3870-3876.
[52] Grinius L, Kessler C, Schroeder J and Handwerger S. Forkhead transcription factor FOXO1A is critical for induction of human decidualization. J Endocrinol 2006; 189: 179-187.
[53] Samuelson LC. Debate over the identity of an intestinal niche-cell population settled. Nature 2018; 558: 380-381.
[54] Salker MS, Nautiyal J, Steel JH, Webster Z, Sucurovic S, Nicou M, Singh Y, Lucas ES, Murakami K, Chan YW, James S, Abdallah Y, Christian M, Croy BA, Mulac-Jericevic B, Quenby S and Brosens JJ. Disordered IL-33/ST2 activation in decidualizing stromal cells prolongs uterine receptivity in women with recurrent pregnancy loss. PLoS One 2012; 7: e52252.
[55] Weimar CH, Kavelaars A, Brosens JJ, Gellersen B, de Vreeden-Elbertse JM, Heijnen CJ and Macklon NS. Endometrial stromal cells of women with recurrent miscarriage fail to discriminate between high-and low-quality human embryos. PLoS One 2012; 7: e41424.
[56] Garrido-Gomez T, Dominguez F, Quiñonero A, Diaz-Gimeno P, Kapidzic M, Gormley M, Ona K, Padilla-Iserte P, McMaster M and Genbacev O. Defective decidualization during and after severe preeclampsia reveals a possible maternal contribution to the etiology. Proc Natl Acad Sci U S A 2017; 114: E8468-E8477.
[57] Gellersen B and Brosens JJ. Cyclic decidualization of the human endometrium in reproductive health and failure. Endocr Rev 2014; 35: 851-905.
[58] Marcellin L, Santulli P, Gogusev J, Lesaffre C, Jacques S, Chapron C, Goffinet F, Vaiman D and Méhats C. Endometriosis also affects the decidua in contact with the fetal membranes during pregnancy. Hum Reprod 2014; 30: 392-405.
[59] Sipos F and Galamb O. Epithelial-to-mesenchymal and mesenchymal-to-epithelial transitions in the colon. World J Gastroenterol 2012; 18: 601-608.
[60] Owusu-Akyaw A, Krishnamoorthy K, Goldsmith LT and Morelli SS. The role of mesenchymal-epithelial transition in endometrial function. Hum Reprod Update 2018; 25: 114-133.
[61] Yun MS, Kim SE, Jeon SH, Lee JS and Choi KY. Both ERK and Wnt/beta-catenin pathways are involved in Wnt3a-induced proliferation. J Cell Sci 2005; 118: 313-322.